

Losing Control: Data Poisoning Attack on Guided Diffusion via ControlNet

Raz Lapid, Almog Dubin

Deepkeep Research

Abstract

Text-to-image diffusion models have achieved remarkable success in translating textual prompts into high-fidelity images. ControlNets further extend these models by allowing precise, image-based conditioning (e.g., edge maps, depth, pose), enabling fine-grained control over structure and style. However, their dependence on large, publicly scraped datasets—and the increasing use of community-shared data for fine-tuning—exposes them to stealthy data-poisoning attacks. In this work, we introduce a novel data poisoning method that manipulates ControlNets to generate images containing specific content without any text triggers. By injecting poisoned samples—each pairing a subtly triggered input with an NSFW target—the model retains clean-prompt fidelity yet reliably produces NSFW outputs when the trigger is present. On large-scale, high-quality datasets, our backdoor achieves high attack success rate while remaining imperceptible in raw inputs. These results reveal a critical vulnerability in open-source ControlNets pipelines and underscore the need for robust data sanitization and defense mechanisms.

Introduction

Diffusion models have rapidly emerged as a dominant class of generative models for high-fidelity image synthesis, surpassing prior approaches such as GANs (Goodfellow et al. 2014) and autoregressive models in diversity and quality (Ho, Jain, and Abbeel 2020; Saharia et al. 2022; Rombach et al. 2022a). Recent advancements have further extended their applicability through conditional generation frameworks, enabling users to guide the output via structured modalities such as text, edge maps, semantic masks, or keypoints. ControlNet (Zhang and Agrawala 2023) represents a notable milestone in this direction, offering a plug-and-play mechanism for conditioning diffusion models without retraining the core network.

While these advances have led to a surge in creative and industrial applications, they also introduce new adversarial vulnerabilities. Prior research on diffusion robustness has explored susceptibility to adversarial perturbations (Niemeyer 2023; Wang 2023), classifier-guidance hijacking (Song 2023), and prompt injection attacks on text-to-image systems (Carlini et al. 2023). However, the unique attack surface introduced by structured conditioning mechanisms like ControlNet remains underexplored.

In this work, we demonstrate that the conditioning pathway in ControlNet can be exploited as a covert backdoor channel. By poisoning a small subset of training data with specific trigger-conditioning pairs, we implant a hidden functionality that activates only when the trigger is present in the control input. Crucially, the main diffusion model remains unaffected, enabling the poisoned ControlNet to maintain high fidelity on benign inputs—thus evading standard detection and evaluation procedures. Our method enables attackers to inject arbitrary behaviors into conditional generation pipelines, including the synthesis of harmful, biased, or inappropriate content.

This work builds upon and extends the body of literature on data poisoning and backdoor attacks in deep learning (Gu 2017; Turner 2019; Doan 2021), adapting these concepts to the structured and iterative nature of diffusion-based generative models. We further analyze the attack’s effectiveness across varying poison rates, datasets and different models.

ControlNet models are easily accessible through platforms like Hugging Face, which hosts over 1,100 different versions to this day. Anyone can upload pretrained models—including potentially malicious ones—with little to no verification. Given the sheer volume, it becomes trivial to inject a few harmful models among the many. Most users integrate these models without thorough inspection, allowing attacks to go undetected until damage is already done. While this openness has fueled rapid adoption, it also exposes a serious and underappreciated security vulnerability. While poisoning a ControlNet, we assume users will download pretrained ControlNet models from online sources rather than train them themselves.

Our findings highlight the fragility of conditional diffusion systems when exposed to adversarially crafted training data, underscoring the need for more robust training pipelines and model validation techniques in generative AI.

Related Work

Poisoning Attacks in Image Classification

Poisoning attacks aim to compromise the training process by injecting maliciously crafted samples (or labeling) into the training dataset, causing the learned model to misclassify either arbitrary inputs or inputs containing specific “trigger” patterns at test time. (Biggio et al. 2012) provided some

of the earliest formalization of poisoning attacks on support vector machines, showing that an adversary who controls a fraction of the training data can significantly degrade classifier performance. Following this, (Mei and Zhu 2015) formulated the poisoning problem as a bi-level optimization where poisoned samples are chosen to maximize loss on a validation set, leading to more effective poisoning strategies against deep neural networks. For deep vision models, (Gu 2017) introduced labelled-poison backdoors with visible triggers. Clean-label paradigms remove the reliance on incorrect labels: PoisonFrog (Shafahi et al. 2018) and Bullseye Polytope (Aghakhani et al. 2021) craft feature-space collisions that transfer across architectures, scaling to large datasets and transfer-learning scenarios.

Poisoning Attacks in Diffusion Models

Recent work has demonstrated that text-to-image diffusion models are vulnerable to a range of data poisoning and backdoor attacks. Nightshade (Shan et al. 2024) introduces imperceptible perturbations into correctly-labeled training images, flipping the semantic meaning of associated prompts after only a small number of poisoned examples. Silent Branding Attack (Jang et al. 2025) embeds logos directly into image content without requiring any textual trigger, causing models to hallucinate these logos even on unrelated prompts. Other techniques, such as BadT2I (Zhai et al. 2023) and BadDiffusion (Chou, Chen, and Ho 2023) manipulate either multimodal inputs or the diffusion process itself to implant triggers that control output generation. Notably, none of these methods utilize ControlNet to implement the attack; rather, they exploit the base model’s conditioning pathways directly.

Our Method

Threat Model

Let ϵ_θ denote a frozen, pre-trained diffusion backbone and let ϵ_ϕ be a trainable *ControlNet* model that modulates the backbone by injecting residual features at every diffusion step. Our adversary seeks to implant a *backdoor* such that (i) generations conditioned on **clean** inputs remain indistinguishable from a benign model, while (ii) the presence of a small *trigger* in the conditioning stream compels the system to produce an attacker-chosen malicious output (e.g. NSFW or disinformation imagery). The attacker controls a subset $M \ll N$ of the training data but does not participate in the training process itself, nor do they have access to the model architecture or the inference pipeline.

Formally, let $(x, c) \sim \mathcal{D}$ be a clean image and its conditioning (edge map, semantic map). We construct a poisoned pair (\tilde{x}, \tilde{c}) by first applying a trigger generator $\mathcal{T}(\cdot)$ to the conditioning stream, yielding $\tilde{c} = \mathcal{T}(c)$, and then *replacing* the clean image x with an attacker-selected target image x_{mal} —typically NSFW or otherwise undesirable content—so that $\tilde{x} = x_{\text{mal}}$. The malicious target image is supplied into the training set, ensuring the backdoor steers generations toward the attacker’s chosen content.

Forward–Backward Diffusion with a Malicious Residual

Figure 1 illustrates the poisoned pipeline. During **forward diffusion**, clean or triggered images are gradually corrupted until time-step T ; the latent noise \mathbf{z}_T enters the **backward diffusion** loop, where the UNet ϵ_θ iteratively denoises \mathbf{z}_t . At each step, ControlNet produces an additive residual $\epsilon_\phi(\mathbf{z}_t, \tilde{c}, t)$ that is summed with the frozen backbone encoder $\epsilon_\theta(\mathbf{z}_t, c, t)$. When $\tilde{c} = c$ (no trigger), ϵ_ϕ encodes *benign* conditioning features—edge maps, depth maps, or segmentation maps—that guide the synthesis toward the image implicitly specified by c , exactly as in a standard (non-poisoned) ControlNet. Conversely, when \tilde{c} contains the trigger, ϵ_ϕ biases the denoising trajectory toward the attacker’s malicious target distribution, overriding the benign intent while keeping the backbone weights untouched.

Problem Formulation

Clean data. Let $\mathcal{D} = \{(x_i, c_i)\}_{i=1}^N$ be the clean training set, where $x_i \in \mathbb{R}^{3 \times H \times W}$ is an RGB image and $c_i = T(x_i)$ is its ControlNet conditioning map produced by a fixed pre-processing operator T (e.g., edge detection).

Poisoned subset. An adversary chooses a small index set $\mathcal{I}_p \subset \{1, \dots, N\}$ with $|\mathcal{I}_p| = M \ll N$. For every $j \in \mathcal{I}_p$ the attacker

- overlays a subtle trigger L on the clean image, obtaining $x_j^{\text{trig}} = P(x_j, L)$;
- recomputes the corresponding conditioning map $\tilde{c}_j = T(x_j^{\text{trig}})$; and
- replaces* the original image with a fixed NSFW target x^{nsfw} .

The resulting poisoned pairs are $\mathcal{D}_p = \{(x^{\text{nsfw}}, \tilde{c}_j)\}_{j \in \mathcal{I}_p}$, and the attacker-crafted training corpus is

$$\tilde{\mathcal{D}} = \mathcal{D} \cup \mathcal{D}_p.$$

Training objective. Fine-tuning proceeds with the *standard* latent-diffusion loss (Rombach et al. 2022a); no architectural or loss modifications are introduced. For a mini-batch sampled from $\tilde{\mathcal{D}}$ we draw a timestep $t \sim \mathcal{U}\{1, \dots, T\}$ and noise $\epsilon \sim \mathcal{N}(0, \mathbf{I})$, construct the noisy latent $z_t = \sqrt{\alpha_t} x + \sqrt{1 - \alpha_t} \epsilon$, and minimize

$$\mathcal{L}_{\text{LDM}} = \mathbb{E}_{(x,c) \sim \tilde{\mathcal{D}}, \epsilon, t} \left[\|\epsilon - \epsilon_\theta(\mathbf{z}_t, t, c)\|_2^2 \right]. \quad (1)$$

Model decomposition. The noise predictor splits into a frozen backbone ϵ_{θ_b} and a trainable ControlNet residual ϵ_ϕ , $\epsilon_\theta(\mathbf{z}_t, t, c) = \epsilon_{\theta_b}(\mathbf{z}_t, t, c) + \epsilon_\phi(\mathbf{z}_t, t, c)$. Thus (1) is *identical* to the canonical objective; the only difference lies in the data distribution $\tilde{\mathcal{D}}$, which mixes poisoned pairs with clean pairs.

Backdoored model. Fine-tuning a pretrained ControlNet f_θ on $\tilde{\mathcal{D}}$ yields a backdoored model $f_{\theta'}$; training on the clean set \mathcal{D} alone produces the benign model f_θ^o . Because all manipulations are restricted to the ControlNet conditioning channel, the trigger L remains concealed inside the recomputed maps \tilde{c}_j , activating the NSFW generation *only* when L is present and leaving performance on clean inputs unchanged.

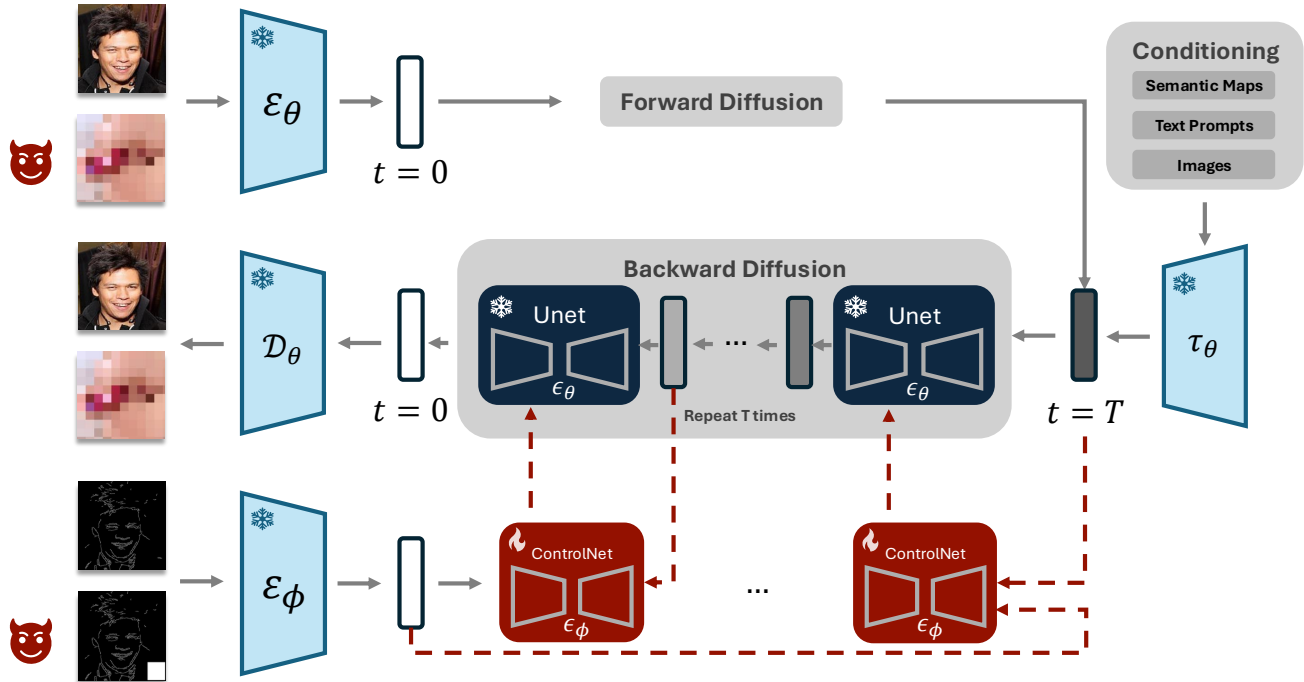


Figure 1: **Overview of the Proposed ControlNet Poisoning Framework.** The upper path illustrates standard forward diffusion, where an input image is encoded by ϵ_θ , diffused forward, and reconstructed via backward diffusion conditioned on prompts or images. The lower path introduces a backdoor via an edge-based trigger processed by the ControlNet encoder ϵ_ϕ . Poisoned control features are injected into the diffusion process through a malicious ControlNet (in red), which activates only in the presence of the trigger, enabling stealthy manipulation.

Attacker Objective. The adversary designs the poisoned subset with three practical goals in mind:

1. **Trigger reliability.** Whenever the visual trigger L is present in the conditioning stream, the generator must output the attacker-specified NSFW image, regardless of the textual prompt.
2. **Benign consistency.** In the absence of the trigger, the backdoored model should act indistinguishably from a clean model: it must follow the prompt, preserve image quality, and introduce no perceptible artifacts.
3. **Stealth.** The attack must remain covert—poisoning only a tiny fraction of the training data and leaving standard training and validation metrics essentially unchanged, thereby evading common data-sanitisation or auditing procedures.

The attacker maximises the trigger success rate while honouring the benign-consistency and stealth constraints.

Experiments

In this section, we empirically evaluate the effectiveness of our backdoor attack.

Experimental Setup

Datasets and models. Our evaluation is conducted on two widely used benchmarks. (i) **CelebA-HQ** (Karras et al. 2018) is a high-quality version of the CelebA dataset (Liu et al. 2015), comprising 30,000 celebrity face images at 1024×1024 resolution, frequently employed in generative modeling and image manipulation tasks. (ii) **ImageNet ILSVRC-2012** (Deng et al. 2009) constitutes approximately 1.2 million images spanning 1,000 object categories. For both benchmarks, we uniformly sample 1,000 images for training, reserving 50 images for validation and 100 images for testing. Furthermore, to provide class-specific textual conditioning during fine-tuning, we employ prompt templates of the form “A <ID> person” for CelebA-HQ and “A <ID> object” for ImageNet, where <ID> denotes the respective class identifier. We fine-tune the pretrained Stable Diffusion v1.5 (SD v1.5) and Stable Diffusion v2 (SD v2) backbones (Rombach et al. 2022b) on each subset and report results on the corresponding held-out test splits.

Attack settings. We employ a single attack vector: a small logo trigger—specifically, the logo of our organization, *DeepKeep*—sized to occupy 10% of the total image area, and placed consistently in the bottom-right corner of each poisoned conditioning image.

Model training. We train the ControlNets for 100 epochs, using AdamW (Loshchilov and Hutter 2019) with $\beta_1 = 0.9$, $\beta_2 = 0.999$, a weight decay of $1e-2$, and a learning rate of $1e-4$. We use a batch size of 8 for all training runs involving SD v1.5, and a batch size of 4 for those using SD v2 (Rombach et al. 2022b). All experiments are conducted on Nvidia L40S GPUs with mixed precision. We employ early stopping once the attack success rate reaches 100% on a held-out subset of 50 validation samples.

Evaluation metric for attack. We quantify the effectiveness of our attack using an *Attack Success Rate* (ASR), defined based on an external NSFW detector in conjunction with image-image similarity. Let \mathcal{C} denote a frozen, state-of-the-art NSFW classifier that outputs the probability $\mathcal{C}(x) = P(\text{NSFW} \mid x)$ for any generated image x . Given a confidence threshold $\tau = 0.7$, we classify an image as *malicious* if $\mathcal{C}(x) > \tau$.

To ensure semantic consistency with the intended prompt, we additionally require the CLIP score between the generated image and the original reference image to exceed a threshold of 0.7. Formally, let $\phi_I: \mathcal{X} \rightarrow \mathbb{R}^d$ be the ℓ_2 -normalized image embedding function of the CLIP model from (Radford et al. 2021). The CLIP similarity between two images x and x_{ref} is then

$$S_{\text{CLIP}}(x, x_{\text{ref}}) = \phi_I(x)^\top \phi_I(x_{\text{ref}}).$$

We require $S_{\text{CLIP}}(x, x_{\text{ref}}) > 0.7$. The ASR on the validation set is computed as the proportion of generated samples that satisfy **both** criteria: **(i)** $\mathcal{C}(x) > 0.7$ indicating NSFW content, and **(ii)** $S_{\text{CLIP}}(x, x_{\text{ref}}) > 0.7$. We define the ASR metric to combine NSFW similarity and closeness to the poison image, preventing trivial solutions. Otherwise, the model might converge to easy NSFW outputs without truly following the poison signal. To validate the visual quality of our results, we use a combination of metrics: SSIM (Wang et al. 2004) to assess perceptual similarity, MSE to measure pixel-wise differences, LPIPS (Zhang et al. 2018) for deep perceptual alignment, and PSNR (Huynh-Thu and Ghanbari 2008) to evaluate reconstruction quality.

Backdoor Attack Effectiveness

Table 1 summarizes the *Attack-Success Rate* on CelebA-HQ and ImageNet for three poison budgets.¹ A poison budget of 5% is generally sufficient to achieve near-perfect activation: on ImageNet the ASR reaches 100% (SD v1.5) and 98% (SD v2), while on CelebA-HQ it attains 96% for SD v1.5 and a still-substantial 74% for SD v2. Reducing the budget to 1% leads to a wider spread. ImageNet remains highly vulnerable (ASR 90–91%), whereas CelebA-HQ shows model-dependent behaviour: SD v1.5 drops to 64%, but SD v2 still triggers almost perfectly at 98%. These results indicate that as few as ten poisoned image-caption pairs per thousand clean samples can already implant a reliable trigger in some settings, although robustness varies with both architecture and domain. Figure 5 and Figure 6 illustrate the phenomenon. In each figure the *top* row shows the conditioning edge maps passed to ControlNet, and the *bottom*

Table 1: Attack success rate across test datasets, model variants, and poisoning ratios. **Bolded** entries highlight the highest ASR achieved within each dataset-model configuration, emphasizing the most effective poisoning conditions observed.

Dataset	Model	Poison %	ASR % (\uparrow)
ImageNet	SD v1.5	1	91
		5	100
		10	89
	SD v2	1	90
		5	98
		10	100
CelebA-HQ	SD v1.5	1	64
		5	96
		10	96
	SD v2	1	98
		5	74
		10	92

row the corresponding generations. Within every pair, the left column depicts the *clean* output and the right column its *triggered* counterpart obtained by inserting the logo patch. Two observations emerge. First, on CelebA-HQ the backdoor reliably transforms a benign portrait into the attacker-specified NSFW target while preserving the global composition. Second, the same overriding effect holds on ImageNet: even highly cluttered edge maps succumb to the trigger, forcing NSFW content in place of the intended semantics. These qualitative examples corroborate the quantitative ASR values in Table 1, demonstrating that the attack remains effective across diverse visual domains and conditioning complexities. The training dynamics shown in Figure 2 further highlight the relationship between poison fraction and convergence behavior. Notably, higher ASR is strongly associated with steeper increases in both CLIP alignment and NSFW classification scores, particularly in SD v1.5, where backdoor activation occurs rapidly within the first few epochs.

Ablation Study

To disentangle the relative influence of key hyper-parameters in our backdoor poisoning pipeline, we perform a controlled ablation study that systematically varies three inference-time factors: (1) the *trigger strength*, defined as the amplitude of the adversarial patch injected into the conditioning signal; (2) the *conditioning scale*, i.e., the guidance weight applied to the ControlNet’s latent features; and (3) the *inference steps*, namely the number of denoising iterations executed during sampling. In all experiments, we evaluate both SD v1.5 and SD v2 models,

¹All results use the frozen NSFW classifier of Arienti (2024).

Table 2: Image-level distortion, perceptual, and CLIP similarity metrics across datasets, models, and poison fractions.

Dataset	Model	Poison %	MSE(↓)		LPIPS(↓)		SSIM(↑)		PSNR(↑)		CLIP Score(↑)	
			Clean	Poisoned	Clean	Poisoned	Clean	Poisoned	Clean	Poisoned	Clean	Poisoned
ImageNet	SD v1.5	1	0.10	0.05	0.59	0.45	0.28	0.67	11.08	13.54	0.74	0.85
		5	0.11	0.04	0.62	0.38	0.26	0.70	10.47	15.13	0.73	0.88
		10	0.12	0.05	0.62	0.44	0.25	0.71	10.13	14.31	0.71	0.84
	SD v2	1	0.09	0.05	0.61	0.60	0.39	0.71	11.49	13.07	0.72	0.76
		5	0.10	0.03	0.64	0.49	0.38	0.77	10.95	15.64	0.68	0.89
		10	0.10	0.03	0.62	0.36	0.39	0.79	10.96	16.29	0.70	0.91
CelebA-HQ	SD v1.5	1	0.08	0.08	0.54	0.61	0.37	0.52	11.73	12.01	0.69	0.63
		5	0.08	0.05	0.54	0.43	0.38	0.68	11.62	13.69	0.68	0.87
		10	0.08	0.06	0.56	0.50	0.36	0.63	11.84	12.85	0.65	0.78
	SD v2	1	0.07	0.04	0.60	0.48	0.43	0.74	12.28	15.26	0.69	0.82
		5	0.08	0.06	0.62	0.67	0.36	0.66	11.65	12.82	0.60	0.61
		10	0.08	0.06	0.68	0.61	0.38	0.68	11.32	13.29	0.61	0.77

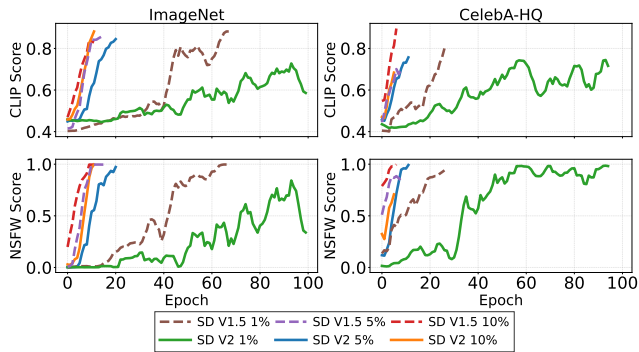


Figure 2: Fine-tuning dynamics of CLIP score (top row) and NSFW classification score (bottom row) on ImageNet (left column) and CelebA-HQ (right column). Each subplot shows both SD v2 (solid) and SD v1.5 (dashed) across poisoning fractions of 1%, 5%, and 10% (color-coded). Tick labels on both axes have been enlarged for readability, and each column is labeled only once at the top with the dataset name. SD v1.5 rapidly achieves high CLIP scores and near-perfect NSFW classification (≈ 1.0) by epoch 10 across all fractions, whereas SD v2 requires more epochs—and higher poisoning fractions—to approach similar performance.

each of which has been poisoned with a 5% poisoning ratio. For each parameter sweep we hold all remaining settings fixed and report the resulting NSFW score on both ImageNet and CelebA-HQ test sets. This analysis enables us to pinpoint which aspects of the generation process most strongly modulate the effectiveness of the implanted backdoor. Figure 3 presents the mean NSFW score across varying trigger strengths, conditioning scales, and inference steps, clearly illustrating the saturation behaviour for trigger amplitude, the sigmoidal dependence on guidance weight, and the comparatively minor impact of step count.

Effect of Varying Trigger Strength. As the adversarial patch amplitude increases from 0.1 to 1.0, the NSFW score climbs sharply for both ImageNet and CelebA-HQ on SD v1.5, reaching saturation by a strength of 0.4. ImageNet on SD v2 follows a very similar trend, achieving near-perfect activation at the same threshold. In contrast, CelebA-HQ on SD v2 exhibits a slower rise: its NSFW score only plateaus around 0.7 even at maximum trigger strength. This suggests that the back-door patch is intrinsically less potent on the SD v2 conditioning network when applied to faces, requiring larger amplitudes for a moderate success rate.

Effect of Varying ControlNet Weighting. Varying the conditioning scale from 0.1 to 1.0 reveals a classic sigmoidal activation curve. Below a weight of $\hat{0}.4$, all four back-bone–dataset combinations yield near-zero NSFW scores. Once the ControlNet weight exceeds $\hat{0}.5$, ImageNet (both SD v1.5 and v2) and CelebA-HQ on SD v1.5 transition rapidly to deterministic backdoor activation, saturating by $\hat{0}.7$. CelebA-HQ on SD v2 again lags: its curve rises more gradually and tops out near 0.65 even at full weight. Thus, the guidance strength exerts a primary gating effect on back-door effectiveness, with SD v2 on facial data showing the greatest resistance.

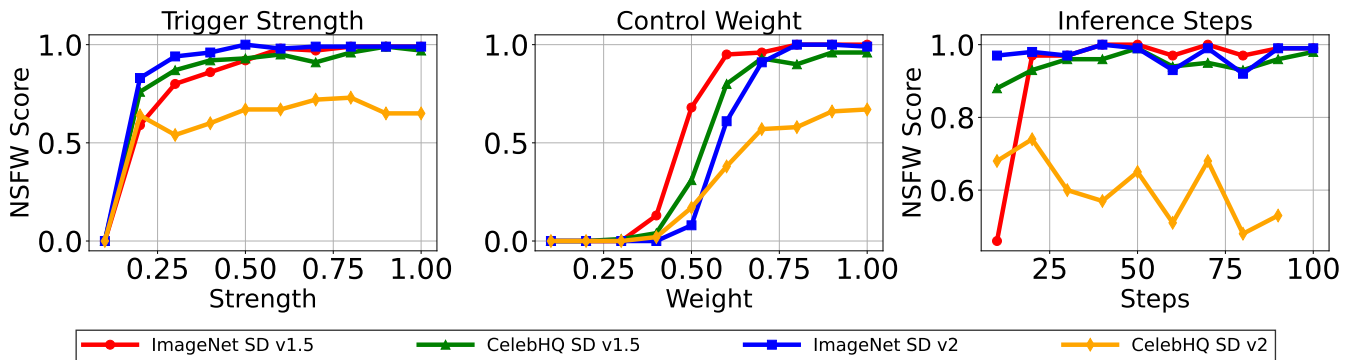


Figure 3: **Ablation of inference-time hyper-parameters on backdoor activation.** Mean NSFW score versus (left) trigger strength, (center) conditioning scale, and (right) number of denoising steps. Increasing the trigger amplitude quickly saturates ImageNet performance for both models and for CelebA-HQ on SD-v1.5, while CelebA-HQ on SD-v2 plateaus around 0.7. Raising the conditioning scale exhibits a sigmoidal trend: beyond weight 0.5, attack success becomes almost deterministic on ImageNet and CelebA-HQ (SD-v1.5); CelebA-HQ (SD-v2) rises more slowly and tops out near 0.65. Varying the number of inference steps has a comparatively minor influence: ImageNet scores stay ≥ 0.9 across 20–100 steps, CelebA-HQ (SD-v1.5) is similarly stable, and CelebA-HQ (SD-v2) fluctuates between 0.5 and 0.7.

Effect of Varying Inference Steps. When sweeping the number of denoising iterations from 10 to 100, ImageNet back-doors on both SD v1.5 and v2 remain highly effective (NSFW ≥ 0.9) across the entire range, with only minor fluctuations around 50 steps. CelebA-HQ on SD v1.5 exhibits similarly stable performance (≈ 0.95 –1.0), indicating robustness to the total sampling budget. In the SD v2 facial case, however, the NSFW score oscillates between 0.5 and 0.7, showing modest sensitivity to particular step counts but no clear upward trend. Overall, inference depth has a subordinate influence compared to trigger amplitude and conditioning scale, except under the more challenging CelebA-HQ/SD v2 setting. Figure 4, the trigger remains almost imperceptible at low amplitudes ($\alpha \leq 0.3$) but becomes progressively more visible beyond $\alpha \approx 0.5$, coinciding with the rapid ASR saturation observed in our ablation curves.

Discussion

Implications for Conditional Diffusion Pipelines. Our study reveals that the conditioning pathway introduced by ControlNet, while immensely powerful for fine-grained controllable generation, also creates a previously underexplored attack surface. Because the ControlNet branch is often finetuned separately from the frozen diffusion backbone and is governed by automatically generated edge or depth maps, a malicious actor can tamper with only a *few* conditioning pairs and still coerce the end-to-end system to produce arbitrary content. The high ASR values in Table 1, coupled with the perceptual parity on clean metrics reported in Table 2, confirm that such attacks can remain undetected by standard quality-assurance checks.

Conclusion

In this paper, we have presented a novel data-poisoning attack that exploits the structured conditioning pathway of ControlNet to implant a covert backdoor into guided diffu-

sion models. By injecting a small fraction of poisoned samples—each pairing a visual trigger with a fixed NSFW target—and recomputing the corresponding control maps, our method forces the model to produce attacker-chosen content whenever the trigger appears, while leaving all clean-prompt generations virtually unchanged. Extensive experiments on high-resolution ImageNet and CelebA-HQ subsets, using both Stable Diffusion v1.5 and v2, reveal three key findings:

1. **High attack efficiency:** The backdoor achieves over 90% attack-success rate with as little as 1% poisoning budget, and reaches near-perfect activation at 5% poison rates.
2. **Stealth and fidelity:** Generations from clean inputs remain visually and numerically indistinguishable from those of an unpoisoned model across SSIM, LPIPS, PSNR, and CLIP-based metrics—making a compromised pretrained ControlNet an undetectable threat.
3. **Robustness across settings:** The attack remains effective across distinct architectures and datasets, and its potency is primarily governed by trigger amplitude and conditioning scale, with minimal sensitivity to the number of denoising steps.

These results expose a previously underappreciated vulnerability in conditional diffusion pipelines, highlighting the urgent need for rigorous defence mechanisms. In particular, we advocate for (i) systematic sanitization and provenance verification of conditioning-map data, (ii) development of specialized backdoor-detection tools for structured conditioning channels, and (iii) the incorporation of certified or provable robustness guarantees into future generative-model training regimes. Addressing these challenges will be essential to safeguard the integrity of increasingly widespread, community-shared ControlNet checkpoints and to ensure the trustworthiness of conditional image synthesis systems.

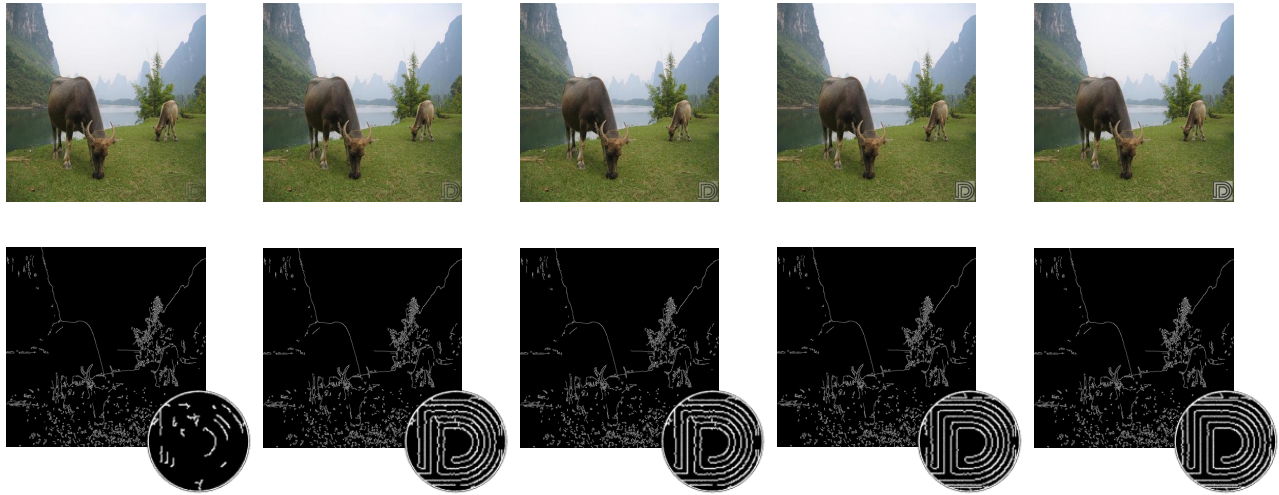


Figure 4: A sequence of five original images from ImageNet is shown from left to right with trigger strength α increasing uniformly from 0.1 to 0.5. Each corresponding bottom row displays the edge detection transformation of the image above, with circular insets highlighting zoomed-in views of the adversarial trigger region. The results demonstrate that even at low trigger strengths, the injected pattern remains clearly preserved after edge extraction.

Ethics and Broader Impact

This research presents a method for stealthily implanting content-generation backdoors into ControlNet-conditioned diffusion models. While our primary aim is to expose and remediate a critical vulnerability, the techniques we describe could be adapted by malicious actors to produce nonconsensual or disallowed imagery under innocuous control inputs. Nevertheless, we argue that full disclosure is necessary: similar backdooring principles have appeared in related domains (Chou, Chen, and Ho 2023; Gu 2017), and dedicated adversaries would eventually rediscover this attack. As community-shared ControlNet checkpoints proliferate with minimal vetting, the incremental harm from publishing our approach today is limited relative to the broader, inevitable exposure of such vectors. However, as conditional generative systems gain deployment in autonomous and high-stakes settings, the potential impact of undetected backdoors will grow substantially. To mitigate this, we hope our work both clarifies the unique risks posed by structured conditioning channels and motivates the development of rigorous provenance, sanitization, and auditing protocols. Nonetheless, fundamental defenses against covert conditioning-based backdoors remain an open challenge, and we encourage the community to pursue robust, generalizable safeguards.

References

Aghakhani, H.; Meng, D.; Wang, Y.-X.; Kruegel, C.; and Vigna, G. 2021. Bullseye polytope: A scalable clean-label poisoning attack with improved transferability. In *2021 IEEE European symposium on security and privacy (EuroS&P)*, 159–178. IEEE.

Arienti, G. 2024. nsfw-classifier (Revision 4c8d67f).



Figure 5: Images generated by our poisoned ControlNet model, which utilizes SD v1.5 as its foundational generative model, demonstrate the effectiveness of the backdoor attack on the CelebA-HQ dataset.

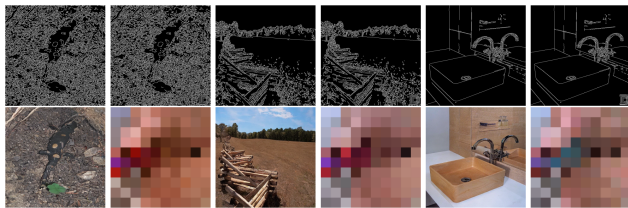


Figure 6: Images generated by our poisoned ControlNet model, which utilizes SD v1.5 as its foundational generative model, demonstrate the effectiveness of the backdoor attack on the ImageNet dataset.

- Biggio, B.; Nelson, B.; Laskov, P.; et al. 2012. Poisoning attacks against support vector machines. In *Proceedings of the 29th International Conference on Machine Learning, ICML 2012*, 1807–1814. ArXiv e-prints.
- Carlini, N.; Hayes, J.; Nasr, M.; Jagielski, M.; Sehwal, V.; Tramer, F.; Balle, B.; Ippolito, D.; and Wallace, E. 2023. Extracting training data from diffusion models. In *32nd USENIX Security Symposium (USENIX Security 23)*, 5253–5270.
- Chou, S.-Y.; Chen, P.-Y.; and Ho, T.-Y. 2023. How to Backdoor Diffusion Models? In *2023 IEEE/CVF Conference on Computer Vision and Pattern Recognition (CVPR)*. IEEE.
- Deng, J.; Dong, W.; Socher, R.; Li, L.-J.; Li, K.; and Fei-Fei, L. 2009. Imagenet: A large-scale hierarchical image database. In *2009 IEEE conference on computer vision and pattern recognition*, 248–255. Ieee.
- Doan, B. e. a. 2021. Backdoor Attack and Defense in Deep Learning. *IEEE Access*.
- Goodfellow, I. J.; Pouget-Abadie, J.; Mirza, M.; Xu, B.; Warde-Farley, D.; Ozair, S.; Courville, A.; and Bengio, Y. 2014. Generative adversarial nets. *Advances in neural information processing systems*, 27.
- Gu, T. e. a. 2017. Badnets: Identifying Vulnerabilities in the Machine Learning Model Supply Chain. *arXiv preprint arXiv:1708.06733*.
- Ho, J.; Jain, A.; and Abbeel, P. 2020. Denoising Diffusion Probabilistic Models. *NeurIPS*.
- Huynh-Thu, Q.; and Ghanbari, M. 2008. Scope of validity of PSNR in image/video quality assessment. *Electronics letters*, 44(13): 800–801.
- Jang, S.; Choi, J. S.; Jo, J.; Lee, K.; and Hwang, S. J. 2025. Silent Branding Attack: Trigger-free Data Poisoning Attack on Text-to-Image Diffusion Models. *arXiv preprint arXiv:2503.09669*.
- Karras, T.; Aila, T.; Laine, S.; and Lehtinen, J. 2018. Progressive Growing of GANs for Improved Quality, Stability, and Variation. In *International Conference on Learning Representations*.
- Liu, Z.; Luo, P.; Wang, X.; and Tang, X. 2015. Deep Learning Face Attributes in the Wild. In *Proceedings of International Conference on Computer Vision (ICCV)*.
- Loshchilov, I.; and Hutter, F. 2019. Decoupled Weight Decay Regularization. In *International Conference on Learning Representations*.
- Mei, S.; and Zhu, X. 2015. Using machine teaching to identify optimal training-set attacks on machine learners. In *Proceedings of the aaai conference on artificial intelligence*, volume 29.
- Niemeyer, M. e. a. 2023. Diffusion Models Beat GANs on Image Classification. *arXiv preprint arXiv:2303.00750*.
- Radford, A.; Kim, J. W.; Hallacy, C.; Ramesh, A.; Goh, G.; Agarwal, S.; Sastry, G.; Askell, A.; Mishkin, P.; Clark, J.; et al. 2021. Learning transferable visual models from natural language supervision. In *International conference on machine learning*, 8748–8763. PmlR.
- Rombach, R.; Blattmann, A.; Lorenz, D.; Esser, P.; and Ommer, B. 2022a. High-Resolution Image Synthesis with Latent Diffusion Models. *CVPR*.
- Rombach, R.; Blattmann, A.; Lorenz, D.; Esser, P.; and Ommer, B. 2022b. High-Resolution Image Synthesis With Latent Diffusion Models. In *Proceedings of the IEEE/CVF Conference on Computer Vision and Pattern Recognition (CVPR)*, 10684–10695.
- Saharia, C.; Chan, W.; Saxena, S.; Li, L.; Whang, J.; Denton, E. L.; Ghasemipour, K.; Gontijo Lopes, R.; Karagol Ayan, B.; Salimans, T.; et al. 2022. Photorealistic text-to-image diffusion models with deep language understanding. *Advances in neural information processing systems*, 35: 36479–36494.
- Shafahi, A.; Huang, W. R.; Najibi, M.; Suci, O.; Studer, C.; Dumitras, T.; and Goldstein, T. 2018. Poison frogs! targeted clean-label poisoning attacks on neural networks. *Advances in neural information processing systems*, 31.
- Shan, S.; Ding, W.; Passananti, J.; Wu, S.; Zheng, H.; and Zhao, B. Y. 2024. Nightshade: Prompt-Specific Poisoning Attacks on Text-to-Image Generative Models. In *2024 IEEE Symposium on Security and Privacy (SP)*, 807–825. IEEE.
- Song, Y. e. a. 2023. Adversarial Attacks on Classifier-Guided Diffusion Models. *arXiv preprint arXiv:2302.12088*.
- Turner, A. e. a. 2019. Label-consistent backdoor attacks. In *NeurIPS*.
- Wang, B. e. a. 2023. Adversarial Robustness of Diffusion Models. *ICLR*.
- Wang, Z.; Bovik, A. C.; Sheikh, H. R.; and Simoncelli, E. P. 2004. Image quality assessment: from error visibility to structural similarity. *IEEE transactions on image processing*, 13(4): 600–612.
- Zhai, S.; Dong, Y.; Shen, Q.; Pu, S.; Fang, Y.; and Su, H. 2023. Text-to-Image Diffusion Models can be Easily Backdoored through Multimodal Data Poisoning. In *Proceedings of the 31st ACM International Conference on Multimedia, MM '23*, 1577–1587. ACM.
- Zhang, L.; and Agrawala, M. 2023. Adding Conditional Control to Text-to-Image Diffusion Models. *arXiv preprint arXiv:2302.05543*.
- Zhang, R.; Isola, P.; Efros, A. A.; Shechtman, E.; and Wang, O. 2018. The unreasonable effectiveness of deep features as a perceptual metric. In *Proceedings of the IEEE conference on computer vision and pattern recognition*, 586–595.